Available online at www.sciencedirect.com
SCIENCE DIRECT®
PERGAMON
Polyhedron 22 (2003) 419–431
POLYHEDRON
www.elsevier.com/locate/poly

Pyrimidine, pyridazine, quinazoline, phthalazine, and triazine coordination polymers of copper(I) halides

Jonathan T. Maeyer [a], T. Jason Johnson [a], Amy K. Smith [a], Brian D. Borne [a], Robert D. Pike [a,*], William T. Pennington [b], Mariusz Krawiec [b], Arnold L. Rheingold [c]

[a] Department of Chemistry, College of William and Mary, Williamsburg, VA 23187, USA
[b] Department of Chemistry, Clemson University, Clemson, SC 29634, USA
[c] Department of Chemistry and Biochemistry, University of Delaware, Newark, DE 19716, USA

Received 19 August 2002; accepted 30 October 2002

Abstract

The coordination of diazine and triazine bridging ligands (B = pyrimidine (Pym), quinazoline (Qnz), pyridazine (Pdz), phthalazine (Ptz), and 1,3,5-triazine (Trz)) with CuX and CuXL (X = Cl, Br, I; L = PPh_3, $P(OPh)_3$) has been investigated. Products without phosphorus(III) ligands include [CuXB] (B = Qnz, Pdz, Ptz), $[(CuX)_2B]$ (B = Pym, Qnz, Pdz, Ptz, Trz), $[(CuX)_3B_2]$ (B = Ptz, Trz), and $[(CuX)_3B]$ (B = Trz). Only CuX–Trz and CuI–Pdz afford more than one product stoichiometry. Products with phosphorus ligands are of the types [(CuXL)B] (B = Pdz, Ptz), $[(CuXL)_2B]$ (B = Pym, Qnz, Pdz, Ptz, Trz), and $[(CuXL)_3B]$ (B = Trz). Thermogravimetic analyses of the complexes typically show step-wise losses of B and L, ultimately yielding CuX. The X-ray crystal structure of [CuBr(Qnz)] features copper atoms bridged by Br and Qnz, forming 2D sheets of fused rectangular $Cu_4Br_2(Qnz)_2$ units. The X-ray structures of $[(CuBr(PPh_3))_2B]$ (B = Pym, Trz) show 1D chains formed from rhomboidal $(CuL)_2Br_2$ units linked by the B ligand. The structure of $[CuCl(PPh_3)(Pdz)]$ is shown by X-ray to be a simple halide-bridged dimer. The X-ray structure of $[(CuCl(P(OPh)_3))_3(Trz)]$ is a hexamer, having an oblate spheroid core. The core is composed of a Cu_6Cl_6 macrocycle capped with two Trz ligands.

Keywords: Copper complexes; Crystal structures; Pyridazine ligands; Pyrimidine ligands; Thermogravimetric analysis; Triazine ligands

1. Introduction

Recently, we [1] and others [2–4] have demonstrated that copper(I) halides undergo self-assembly reactions with bridging nitrogen ligands to produce metal-organic polymers. Copper(I) halides (CuX) are notable for their ability to form rhomboid Cu_2X_2 dimers, Cu_4X_4 cubane tetramers, $(Cu_2X_2)_n$ stair step polymers, and $(CuX)_n$ chains. These structures are linked together by bridging aromatic nitrogen ligands (B), such as pyrazine (Pyz) and 4,4′-bipyridine (Bpy), into a variety of polymeric arrays. The most commonly encountered stoichiometries are 1:1 CuXB and 2:1 $(CuX)_2B$. Multiple three-dimensional (3D) atom arrangements can exist for a given stoichiometry. Additionally, the use of monodentate 'capping' ligands (L) has been shown to limit polymer growth, lowering the dimensionality of the metal-organic polymer, e.g. 2D → 1D [1,5].

In the current contribution, we report the products resulting from the reactions of the B ligands shown in Chart 1 with CuX = CuCl, CuBr, and CuI, in the absence or in the presence of L = PPh_3 and $P(OPh)_3$. These ligands are notable for their geometrically rigid bridging angles of 120 or 60°. Kromp and Sheldrick have reported the binary complexes of pyridazine and pyrimidine: [CuX(Pdz)] (X = Cl, Br, I), $[(CuI)_2(Pdz)]$ and [CuBr(Pym)] [3]. Hubberstey and coworkers have described $[(CuX)_3(Trz)]$ and $[(CuX)_2(Trz)]$ (X = Br, I) [4]. All of the aforementioned species form metal-organic networks. In addition, halide-free networks of

* Corresponding author. Tel.: +1-757-221-2555; fax: +1-757-221-2715.
E-mail address: rdpike@wm.edu (R.D. Pike).

0277-5387/02/$ - see front matter
PII: S0277-5387(02)01372-4

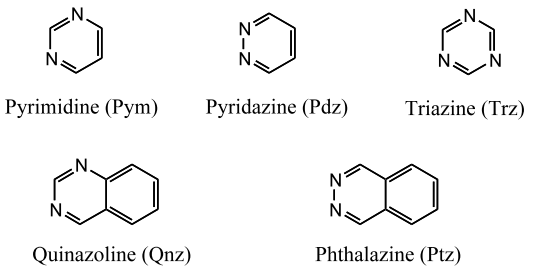

Chart 1.

these ligands are known, including [CuSCN(Pym)] [6], [CuCN(Pdz)] [7] $[Cu(Pym)_2]BF_4$ [8] dimeric $[Cu_2(Pdz)_x(cnge)_2]BF_4$ ($x = 2$, 3; cnge = 2-cyanoguanidine) [9] and $[Cu_2(Pdz)_3(NCMe)_2](PF_6)_2$ and tetrameric $[Cu_4(Pdz)_6](ClO_4)_4$ [10]. No copper(I) halide complexes of Qnz or Ptz have yet been reported. Also novel are the phosphorus(III) adducts of CuX–B.

2. Experimental

2.1. General methods

All syntheses were carried out under nitrogen atmosphere. Microanalyses for C, H, and N were carried out by Atlantic Microlab, Inc., Norcross, GA. Methods used for thermogravimetric analysis (TGA) and atomic absorption analyses have previously been described [1]. All ligands were purchased from Aldrich or Acros and were used as received. Copper(I) chloride and bromide were freshly recrystallized from aq. HCl or HBr. Copper(I) iodide was used as received from Aldrich.

2.2. Syntheses

The following two descriptions are representative of CuX–B and CuX–L–B syntheses, respectively. See Tables 1 and 2 for complete synthetic results.

2.2.1. Synthesis of [CuCl(Qnz)]

Freshly recrystallized CuCl (0.492 g, 4.97 mmol) was dissolved in 40 ml of CH_3CN. The solution was filtered through Celite to remove traces of Cu(II) species, and was stirred under nitrogen at 25 °C. A solution of quinazoline (0.646 g, 4.96 mmol) in 8 ml of $CHCl_3$ was added to the CuCl solution via syringe. A blood red precipitate rapidly developed. After stirring for 30 min at 25 °C, the product was collected via filtration, washed with Et_2O, and then dried under vacuum (0.893 g, 3.90 mmol, 78.6%).

2.2.2. Synthesis of $[(CuI(PPh_3))_2(Pdz)]$

Copper(I) iodide (0.308 g, 1.62 mmol) and PPh_3 (0.426 g, 1.63 mmol) were co-dissolved in 40 ml of $CHCl_3$ at 25 °C. Pyridazine (0.0680 g, 0.849 mmol) in 3 ml of CH_3CN was added by use of syringe. A yellow solution containing a trace of orange powder resulted. After stirring for 15 min, the orange powder, [CuI(Pdz)],

Table 1
Synthetic and analytical data for CuX-B complexes

Compound	Yield (%)	Color	% (theory)	% (experiment)
$[(CuCl)_2(Pym)]$	67	gold	Cu 45.70	45.87
$[(CuBr)_2(Pym)]$	79	yellow–olive	Cu 34.63	33.93
$[(CuI)_2(Pym)]$	89	bright yellow	Cu 27.57	27.28
			C 10.42	10.59
			H 0.87	0.89
			N 6.08	6.06
[CuCl(Qnz)]	79	brick red	Cu 27.73	27.73
			C 41.93	41.39
			H 2.63	2.81
			N 12.23	12.13
[CuBr(Qnz)]	63	red–orange	Cu 23.23	23.03
$[(CuI)_2(Qnz)]$	81	red–orange	Cu 24.87	25.13
			C 18.80	18.92
			H 1.18	1.26
			N 5.48	5.38
[CuCl(Pdz)]	79	dark red	Cu 35.48	36.38
[CuBr(Pdz)]	88	red–brown	Cu 28.43	27.87
			C 21.49	20.99
			H 1.80	1.72
			N 12.53	12.12
[CuI(Pdz)]	86	orange	Cu 23.49	22.65
			C 17.76	17.83
			H 1.49	1.45
			N 10.36	10.25
$[(CuI)_2(Pdz)]$	95	yellow	Cu 27.57	27.84
			C 10.42	10.51
			H 0.87	0.83
			N 6.08	5.93
$[(CuCl)_3(Ptz)_2]$	64	brown	Cu 34.21	33.78
			C 34.48	34.07
			H 2.17	2.39
			N 10.05	9.81
[CuBr(Ptz)]	62	orange	Cu 23.23	23.02
			C 35.12	35.25
			H 2.21	2.27
			N 10.24	10.35
$[(CuI)_2(Ptz)]$	65	orange	Cu 24.87	24.46
			C 18.80	18.54
			H 1.18	1.09
			N 5.48	5.46
$[(CuCl)_2(Trz)]$	70	amber	Cu 45.54	44.74
$[(CuCl)_3(Trz)]$	78	orange–brown	Cu 50.43	47.45
			C 9.52	9.89
			H 0.80	1.00
			N 11.12	11.16
$[(CuBr)_3(Trz)_2]$	20	red–brown	Cu 32.18	32.20
$[(CuBr)_2(Trz)]$	78	orange	Cu 34.54	35.00
			C 9.79	9.67
			H 0.82	0.92
			N 11.42	10.99
$[(CuBr)_3(Trz)]$	76	red–brown	Cu 37.28	37.19
$[(CuI)_2(Trz)]$	94	bright yellow	Cu 27.51	27.58
			C 7.80	8.12
			H 0.65	0.62
			N 9.10	9.11

Table 2
Synthetic and analytical data for CuX–L–B complexes

Compound	Yield (%)	Color	% (theory)	% (experiment)
$[(CuCl(PPh_3))_2(Pym)]$	89	pale yellow	Cu 15.83	16.35
			C 59.85	60.34
			H 4.24	4.27
			N 3.49	3.17
$[(CuBr(PPh_3))_2(Pym)]$	98	yellow	Cu 14.26	14.64
$[(CuI(PPh_3))_2(Pym)]$	36	bright yellow	Cu 12.90	13.11
			C 48.74	47.87
			H 3.48	3.45
			N 2.84	2.78
$[(CuCl(P(OPh)_3))_2(Pym)]$	42	pale yellow	Cu 14.14	13.53
$[(CuBr(P(OPh)_3))_2(Pym)]$	71	pale yellow	Cu 12.87	12.94
			C 48.64	48.04
			H 3.44	3.57
			N 2.84	3.05
$[(CuCl(PPh_3))_2(Qnz)]$	67	bright orange	Cu 14.90	14.35
$[(CuBr(PPh_3))_2(Qnz)]$	68	yellow–orange	Cu 13.50	13.10
$[(CuI(PPh_3))_8(Qnz)]$	82	golden	Cu 13.98	13.55
			C 48.66	48.07
			H 3.38	3.35
			N 0.75	0.89
$[(CuCl(P(OPh)_3))_2(Qnz)]$	62	pale yellow	Cu 13.40	13.16
$[(CuBr(P(OPh)_3))_2(Qnz)]$	66	yellow	Cu 12.25	12.40
			C 50.93	50.88
			H 3.50	3.50
			N 2.70	2.87
$[(CuCl(PPh_3))_2(Pdz)]$	72	light yellow	Cu 15.83	14.99
			C 59.86	59.20
			H 4.27	4.23
			N 3.49	4.07
$[CuBr(PPh_3)(Pdz)]$	63	yellow–orange	Cu 13.08	13.15
			C 54.39	53.84
			H 3.94	4.08
			N 5.77	5.57
$[CuI(PPh_3)(Pdz)]$	65	yellow–orange	Cu 11.93	12.21
$[CuCl(P(OPh)_3)(Pdz)]$	49	yellow	Cu 12.99	12.55
$[CuBr(P(OPh)_3)(Pdz)]$	69	light yellow	Cu 11.90	12.08
			C 49.50	48.61
			H 3.59	3.52
			N 5.25	5.11
$[(CuCl(PPh_3))_2(Ptz)]$	87	yellow	Cu 14.90	14.75
$[CuBr(PPh_3)(Ptz)]$	71	yellow	Cu 11.86	12.13
			C 58.27	57.53
			H 3.95	3.88
			N 5.23	5.21
$[CuI(PPh_3)(Ptz)]$	89	yellow	Cu 10.90	11.13
$[CuCl(P(OPh)_3)(Ptz)]$	76	yellow–orange	Cu 11.78	11.42
$[(CuBr(P(OPh)_3))_2(Ptz)]$	68	yellow	Cu 12.25	12.96
			C 50.93	49.79
			H 3.50	3.41
			N 2.70	3.11
$[(CuCl(PPh_3))_3(Trz)]$	80	yellow–orange	Cu 16.37	16.39
$[(CuBr(PPh_3))_2(Trz)]$	95	yellow	Cu 14.24	14.13
			C 52.48	52.37
			H 3.73	3.71
			N 4.71	4.65
$[(CuI(PPh_3))_2(Trz)]$	92	pale orange	Cu 12.88	12.80
			C 47.48	46.88
			H 3.37	3.35
			N 4.26	4.21
$[(CuCl(P(OPh)_3))_3(Trz)]$	82	yellow orange	Cu 14.56	14.50
			C 52.30	50.19
			H 3.70	3.64

Table 2 (*Continued*)

Compound	Yield (%)	Color	% (theory)	% (experiment)
			N 3.21	2.99
$[(CuBr(P(OPh)_3))_2(Trz)]$	96	orange	Cu 12.86	12.83
			C 47.38	47.25
			H 3.36	3.36
			N 4.25	4.27
$[(CuI(P(OPh)_3))_3(Trz)]$	65	orange	Cu 12.04	11.77
			C 43.24	44.00
			H 3.06	3.34
			N 2.65	2.79

was collected by filtration and discarded. The filtrate was concentrated to 10 ml and the yellow solid product precipitated upon addition of Et_2O. The product was collected via filtration, washed with Et_2O, and then dried under vacuum (0.521 g, 0.529 mmol, 65.3%).

2.3. X-ray data collection, structure soluitons and refinements

The complexes were crystallized as follows. [CuBr(Qnz)]: equal portions 20 mM Qnz and CuBr in CH_3CN were combined. The resulting yellow solution was allowed to stand overnight, yielding large orange plate crystals. $[(CuBr(PPh_3))_2(Pym)]$, $[(CuBr(PPh_3))_2(Trz)]$, $[CuCl(PPh_3)(Pdz)]$, and $[(CuCl(P(OPh)_3))_3(Trz)]$: saturated solutions of the complexes in $CHCl_3$ were layered with ether in 5 mm tubes. Crystals slowly formed over a period of 2 weeks. The $[CuCl(PPh_3)(Pdz)]$ crystals were grown from a solution of $[(CuCl(PPh_3))_2(Pdz)]$.

Crystals were mounted on glass fibers. Least-squares refinement for all structures was carried out on F^2. For all structures except [CuBr(Qnz)], all measurements were made at -100 ± 1 °C on a Bruker AXS diffractometer, equipped with a SMART APEX CCD detector. Data for [CuBr(Qnz)] were collected at 23 ± 1 °C using a Mercury CCD detector coupled to a Rigaku AFC-8S diffractometer. Initial space group determination was based on a matrix of 60 frames. Data were collected in 10, 20, or 30 s frames. The data were reduced using SAINT+ [11] and empirical absorption correction applied using SADABS [12]. Data for [CuBr(Qnz)] were collected and processed using CRYSTAL CLEAR [13].

Structures were solved using the Patterson method for $[(CuBr(PPh_3))_2(Pym)]$ and $[(CuBr(PPh_3))_2(Trz)]$ and direct methods for the other complexes. Rotational twins were present for $[(CuBr(PPh_3))_2(Trz)]$. The GEMINI program [14] was used on 89 reflections to identify the orientation matrices of the two twins (85 and 15% occupancies). The non-hydrogen atoms were refined anisotropically. Hydrogen atoms were placed in theoretical positions. Structure solution, refinement and the calculation of derived results were performed using the SHELXTL [15] package of computer programs. Details of the X-ray experiments and crystal data are summarized in Table 3. Selected bond lengths and angles are given in Table 4.

3. Results and discussion

3.1. Synthesis and characterization of products

Having previously reported the behavior of copper(I) halides with 'linear' bridges, including Pyz, its benzo-derivative, quinoxaline (Quin), and (Bpy) [1], herein is reported the analogous coordination chemistry of the 'bent' bridging ligands, Pym, Qnz, Pdz, Ptz, and Trz (Chart 1). The addition of the bridging ligand to CuX solutions in CH_3CN produced solid products within a few seconds to a few minutes. In the case of CuX–Trz combinations, the products were soluble in CH_3CN and complete precipitation was ensured through the addition of ether. A list of the CuX–B products prepared is shown in Table 1. Solutions of CuXL were formed by addition of equimolar CuX and L in $CHCl_3$. Subsequent treatment with solutions of B produced solids or formed solutions from which product could be precipitated upon addition of ether. A list of the characterized CuXL–B products is found in Table 2.

The formulations of the new compounds were determined through elemental analysis. These results were confirmed via thermogravimetry and, where possible, X-ray crystallography. For the phosphorus-free complexes of Pym, Qnz, Pdz, and Ptz, 1:1 and 2:1 CuX–B ratios predominated (see Table 1). The pyrimidine species prepared were all novel 2:1 complexes, $[(CuX)_2(Pym)]$ (X = Cl, Br, I). Previously, only one Pym complex of CuX had been reported [3]. This was a 1:1 Pym complex, [CuBr(Pym)], prepared at high temperature. The closely related Qnz ligand afforded new 1:1 products for CuCl and CuBr, and a 2:1 product for CuI. The four previously observed Pdz complexes [CuX(Pdz)] (X = Cl, Br, I) and $[(CuI)_2(Pdz)]$ [3] were identified in the current study. The closely related Ptz ligand yielded three distinct stoichiometries, $[(CuCl)_3(Ptz)_2]$, [CuBr(Ptz)], and $[(CuI)_2(Ptz)]$. The 3:2 ratio has not previously been observed in CuX complexes with

Table 3
Crystal and structure refinement data

Complex	[CuBr(Qnz)]	[(CuBr(PPh$_3$))$_2$(Pym)]	[CuCl(PPh$_3$)(Pdz)]$_2$	[(CuBr(PPh$_3$))$_2$(Trz)]	[(CuCl(P(OPh)$_3$))$_6$(Trz)$_2$]
Empirical formula	$C_8H_6BrCuN_2$	$C_{40}H_{34}Br_2Cu_2N_2P_2$	$C_{44}H_{38}Cl_2Cu_2N_4P_2$	$C_{39}H_{33}Br_2Cu_2N_3P_2$	$C_{116}H_{98}Cl_{12}Cu_6N_6O_{18}P_6$
Formula weight	273.60	891.53	882.70	892.52	2856.64
Temperature (°C)	23	−100	−100	−100	−100
Radiation	Mo Kα ($\lambda = 0.71073$ Å)	Mo Kα ($\lambda = 0.71073$ Å)	Mo Kα ($\lambda = 0.71073$ Å)	Mo Kα ($\lambda = 0.71073$ Å)	Mo Kα ($\lambda = 0.71073$ Å)
Color and habit	orange platelet	Yellow needle	yellow block	yellow needle	orange block
Space group	$Pca2_1$ (#29)	$P\bar{1}$ (#2)	$P\bar{1}$ (#2)	$P\bar{1}$ (#2)	$P\bar{1}$ (#2)
a (Å)	21.752(10)	10.2411(17)	8.4658(7)	10.4465(13)	14.1489(7)
b (Å)	3.876(2)	12.647(2)	9.3699(8)	12.1583(15)	15.7470(8)
c (Å)	9.511(5)	14.897(3)	14.3898(12)	14.7891(18)	29.6572(14)
α (°)	90	98.630(3)	78.967(2)	95.289(2)	76.4330(10)
β (°)	90	99.884(3)	73.6040(10)	103.401(2)	79.5120(10)
γ (°)	90	104.433(3)	64.2990(10)	101.887(2)	72.2260(10)
Volume (Å^3)	801.8(5)	1802.7(5)	983.56(14)	1768.6(4)	6088.5(5)
Z	4	2	1	2	2
ρ_{calc} (g cm^{-3})	2.266	1.642	1.490	1.676	1.558
μ(Mo Kα) (mm^{-1})	7.655	3.517	1.336	3.586	1.438
F(000)	528	892	452	892	2896
Crystal size (mm)	0.45 × 0.3 × 0.1	0.3 × 0.05 × 0.02	0.3 × 0.2 × 0.1	0.5 × 0.05 × 0.05	0.4 × 0.3 × 0.1
Residuals: R; R_w	0.095; 0.154 [a]	0.055; 0.167 [b]	0.030; 0.083 [b]	0.035; 0.087 [b]	0.039; 0.083 [b]
Goodness-of-fit	1.930	1.328	1.132	1.023	1.054

[a] $R = R_1 = \Sigma\ ||F_o| - |F_c||/\Sigma\ |F_o|$ for observed data only. $R_w = wR_2 = \{\Sigma\ [w(F_o^2 - F_c^2)^2]/\Sigma\ [w(F_o^2)^2]\}^{1/2}$ for all data.
[b] $R = \Sigma\ ||F_o| - |F_c||/\Sigma\ |F_o|$ for observed data only. $R_w = \{\Sigma\ [w(F_o^2 - F_c^2)^2]/\Sigma\ [w(F_o^2)^2]\}^{1/2}$ for observed data only.

bridging ligands. An X-ray structure was determined for [CuBr(Qnz)] (see below), however none of the new 2:1 or 3:2 materials was successfully crystallized. In general, more copper-rich materials exhibit systems of fused $(CuX)_n$ rings ($n = 2$ or 3), such as those found in [(CuCl)$_2$(Pyz)] [16], [(CuX)$_2$(Bpy)] (X = Cl, Br, I) [17,18], [(CuI)$_2$(Quin)] [1], [(CuI)$_2$(Pdz)] [3], [(CuX)$_3$(Trz)] (X = Br, I) [4], and [(CuBr)$_2$(Trz)] [4].

The reactions of CuX with triazine provided very complex results. Previously, it has been reported that CuBr and CuI form both 3:1 and 2:1 complexes with Trz [4]. These products were reproduced, with the notable exception of [(CuI)$_3$(Trz)]. In addition, an apparent 3:2 complex, [(CuBr)$_3$(Trz)$_2$], was produced. However, an apparent decoupling of CuBr–Trz mixing stoichiometry to product stoichiometry was noted. For example, the

Table 4
Selected bond distances (Å) and angles (°)

	[CuBr(Qnz)]	[(CuBr(PPh$_3$))$_2$(Pym)]	[CuCl(PPh$_3$)(Pdz)]$_2$	[(CuBr(PPh$_3$))$_2$(Trz)]	[(CuCl(P(OPh)$_3$))$_6$(Trz)$_2$]
Bond distances					
Cu–N	2.116(6), 2.020(6)	2.050(5), 2.056(5)	2.0657(14)	2.065(2), 2.075(2)	2.0583(18)–2.1058(18) [a]
Cu–X	2.451(2), 2.540(2)	2.5053(10), 2.5367(11), 2.5332(10), 2.4987(10)	2.3492(5), 2.4334(5)	2.4846(5), 2.5109(5), 2.5510(6), 2.5353(6)	2.3215(6)–2.4297(6) [b]
Cu–P		2.2100(18), 2.2075(18)	2.1902(5)	2.2136(9), 2.2117(9)	2.1544(6)–2.1629(7) [a]
Cu···Cu	3.876(2)	2.8193(16), 2.9342(16)	2.303	2.8545(8), 3.0348(8)	(>4)
Bond angles					
X–Cu–X	101.88(6)	111.95(3), 108.72(3)	95.058(15)	110.951(16), 106.063(16)	110.41(2)–113.97(2) [a]
X–Cu–N	103.7(4), 97.7(4), 122.8(7), 113.8(7)	102.60(14), 100.51(15), 101.55(14), 103.62(14)	106.62(4), 103.80(4)	102.85(7), 101.41(7), 99.30(7), 101.14(7)	94.07(5)–98.75(5) [b]
N–Cu–N	113.5(2)				
P–Cu–X		107.39(6), 110.01(6), 106.78(6), 110.20(6)	124.678(18), 112.785(17)	110.51(3), 114.52(3), 105.63(3), 111.31(3)	108.31(2)–121.53(2) [b]
P–Cu–N		126.37(15), 123.13(15)	111.19(4)	126.77(7), 120.65(7)	121.97(5)–126.42(5) [a]
Cu–X–Cu	101.88(6)	68.05(3), 71.28(3)	84.942(15)	69.049(16), 73.937(16)	127.81(3)–133.58(3) [a]

[a] Range of six values.
[b] Range of 12 values.

3:2, 2:1, and 3:1 CuBr–Trz products were synthesized from 3:1, 3:2, and 1:1 mixing ratios, respectively. Mixing studies of CuCl with Trz provided a variety of products exhibiting many, often ambiguous, stoichiometric ratios, which also seemed unrelated to the mixing ratio. The situation for CuCl–Trz was further complicated by the relative instability of products toward oxidation.

All of the complexes containing $L = PPh_3$ and $P(OPh)_3$ were novel. Elemental analysis data confirmed three stoichiometric ratios: [(CuXL)B] (1:1:1), $[(CuXL)_2B]$, (2:2:1), and $[(CuXL)_3B]$ (3:3:1). Only the products of $CuI–P(OPh)_3–B$ reactions failed to incorporate B ligand. The 1:1:1 products were found in several instances for B = Pdz and Ptz. An example was demonstrated by X-ray crystallography (see below) to be a rhomboid dimer with terminal B ligands. Examples of 2:2:1 products were obtained for all five B ligands, but appeared to predominate for B = Pym and Qnz. These compounds were shown by X-ray to consist of 1D chains of linked rhomboid dimers. The few 2:2:1 complexes of Pdz and Ptz that were isolated appeared to be metastable. Thus in many cases, recrystallization was found to produce the 1:1:1 material, along with 'CuXL' (which typically exists as a tetramer [19]), according to reaction (1).

$$(CuXL)_2B \rightarrow CuXL + (CuXL)B \quad (1)$$

The 3:3:1 products were found only for B = Trz. A structure of one such complex exhibited an unusual hexameric arrangement. A unique result was the formation of an apparent 8:8:1 complex, $[(CuI(PPh_3))_8(Qnz)]$. This formulation was confirmed by elemental analysis and thermogravimetry. Unfortunately, X-ray quality crystals of this compound could not be grown.

3.2. X-ray crystallography

3.2.1. [CuBr(Qnz)]

The molecular structure and sheet arrangement of [CuBr(Qnz)] are shown in Figs. 1 and 2 and represented schematically in Chart 2. The structure is composed of approximately tetrahedral copper atoms linked along the *c*-direction by Qnz rings and along the *b*-direction by Br atoms to form infinite 2D sheets, which stack along the *a*-axis to complete the structure. π-Stacking is also evident along the *b*-axis. The structure can be regarded as a series of zigzag $(CuBr)_\infty$ polymers, which are cross-linked by Qnz ligands projecting alternately above and below the plane of the sheet. In contrast to the current structure, [CuX(Pdz)] structures are composed of $(CuX)_2$ dimer units linked together by pairs of Pdz ligands, and [CuBr(Pym)] is composed of both chains and dimers [3]. These arrangements are illustrated in Chart 2. The copper–nitrogen bonds in [CuBr(Qnz)] are significantly displaced from coplanarity with the heteroaromatic ring (10.9°–16.9°). The spacing between adjacent sheets corresponds to half of the *a*-cell dimension, about 10.9 Å.

3.2.2. $[(CuBr(PPh_3))_2(Pym)]$, $[(CuBr(PPh_3))_2(Trz)]$

The complexes $[(CuBr(PPh_3))_2(Pym)]$ and $[(CuBr(PPh_3))_2(Trz)]$ were isostructural. Molecular structure diagrams for these molecules are given in Figs. 3 and 4. The complexes are composed of quasi-1D polymer chains. This structural type is similar to that found for 2:2:1 complexes of $CuBr(P(OPh)_3)$ [1], and $CuCl(PPh_3)$ [5], with Pyz and Bpy. Each chain is composed of $(CuL)_2Br_2$ dimers linked by B ligands. The zigzag chains

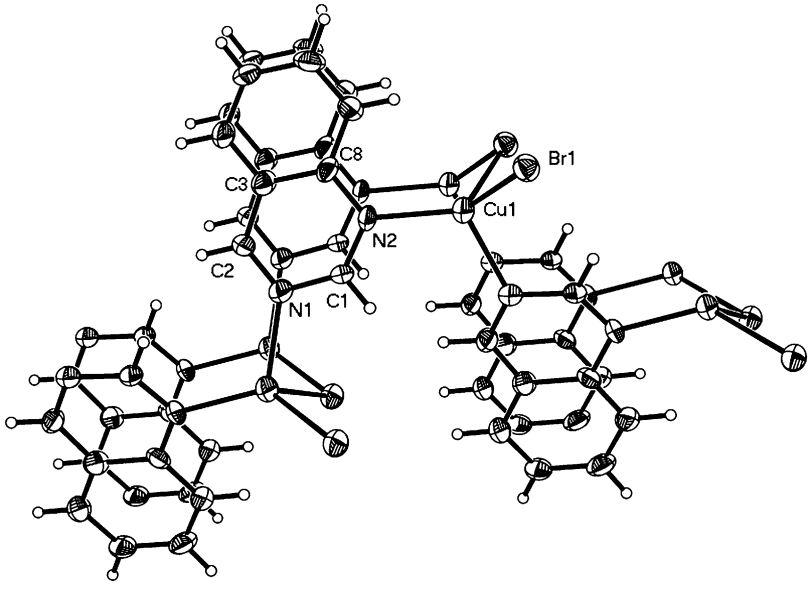

Fig. 1. Molecular structure of [CuBr(Qnz)]. Thermal ellipsoids shown at 50%.

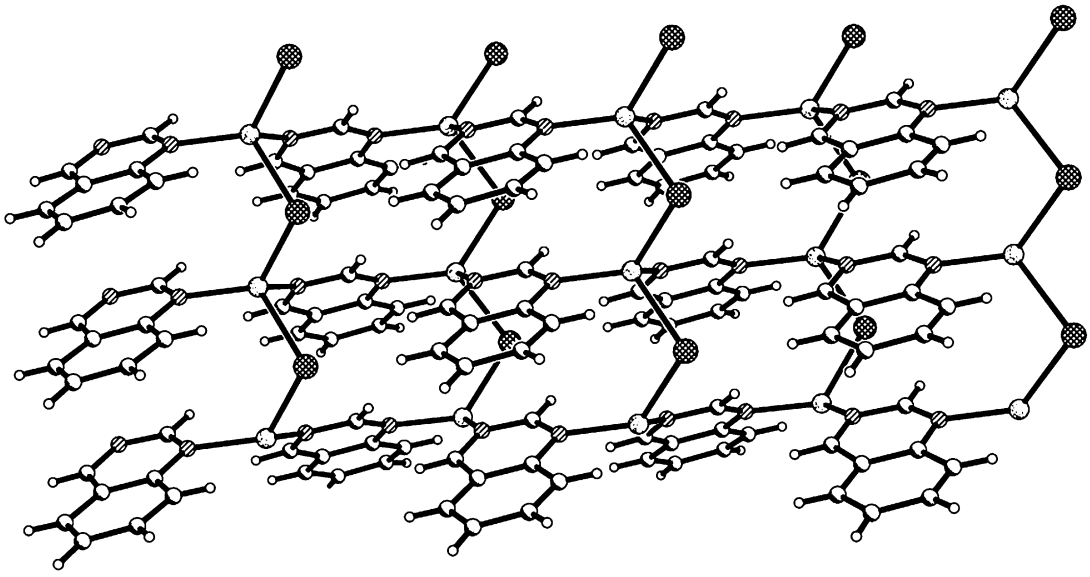

Fig. 2. Sheet arrangement of [CuBr(Qnz)].

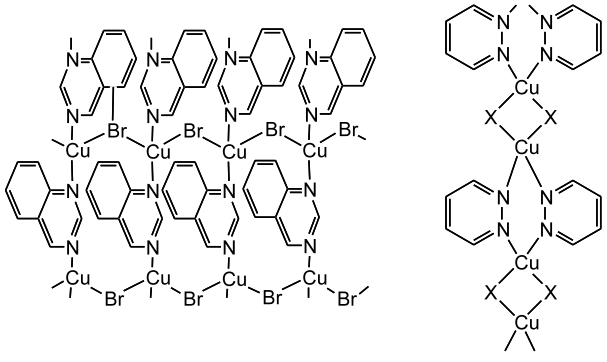

[CuBr(Qnz)]

[CuX(Pdz)]
(X = Cl, Br, I)

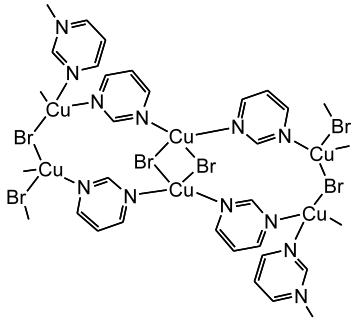

[CuBr(Pym)]

Chart 2.

run parallel to the *c*-axis and pack in the other directions through molecular interactions to complete the structures. The bulky phosphine ligands fill the space on either side of the polymer chains. However, deviations from tetrahedral angles around the copper atoms are relatively small.

3.2.3. *[CuCl(PPh$_3$)(Pdz)]*

Crystallization of the 2:2:1 complex, [(CuCl(PPh$_3$))$_2$(Pdz)] from CHCl$_3$ and ether produced the dimeric 1:1:1 complex, [CuCl(PPh$_3$)(Pdz)] and colorless crystals of [CuCl(PPh$_3$)]$_4$. The molecular structure diagram for the Pdz complex is shown in Fig. 5. The structure reveals monodentate Pdz and PPh$_3$ ligands distributed around a rhomboid Cu$_2$Cl$_2$ core. This arrangement is commonplace in the chemistry of CuX with monodentate ligands [20]. The molecule lies on a crystallographic inversion center. There are no uncharacteristically close contacts or other unusual packing features. This is the first reported Cu(I)–Pdz structure showing monodentate, rather than bidentate, Pdz ligands [3,7,10].

3.2.4. *[(CuCl(P(OPh)$_3$))$_3$(Trz)]*

An X-ray structure of the 3:3:1 complex, [(CuCl(P(OPh)$_3$))$_3$(Trz)] confirmed the expected stoichiometry. However, instead of revealing a polymeric structure, such as those suggested in Chart 3, the hexameric form (Chart 3) was found. A preliminary report of this unique structure has appeared [21]. The molecular structure diagram is presented in Fig. 6. There are two independent molecules located on crystallographic inversion centers in the unit cell. The oblate spheroid molecular core is formed by a puckered 12-membered Cu$_6$Cl$_6$ ring capped by two μ_3-triazine ligands. The core is remarkably symmetrical, showing D_{3d} symmetry and consisting of seven parallel planes: phosphorus, triazine, copper, chloride, copper, triazine and phosphorus. These planes are parallel to one another to within about 1.6°, 2.6° (for the two independent molecules). As is the case for [CuBr(Qnz)], the metal atoms are displaced from the ring plane. In the

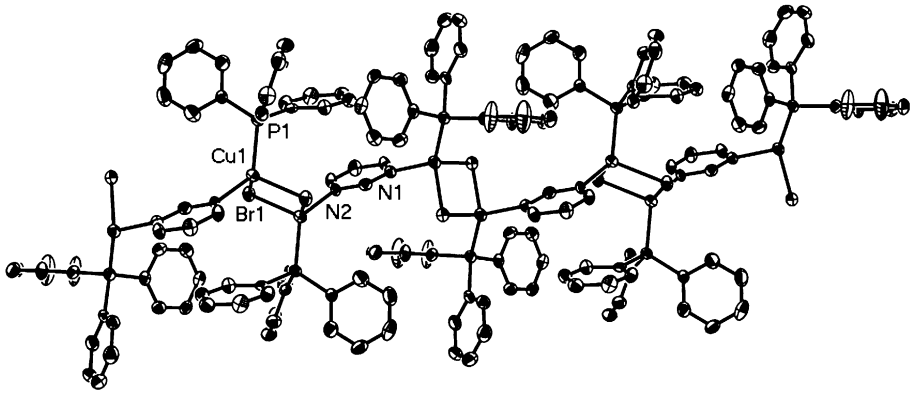

Fig. 3. Molecular structure of $[(CuBr(PPh_3))_2(Pym)]$. Thermal ellipsoids shown at 50%. Hydrogen atoms omitted for clarity.

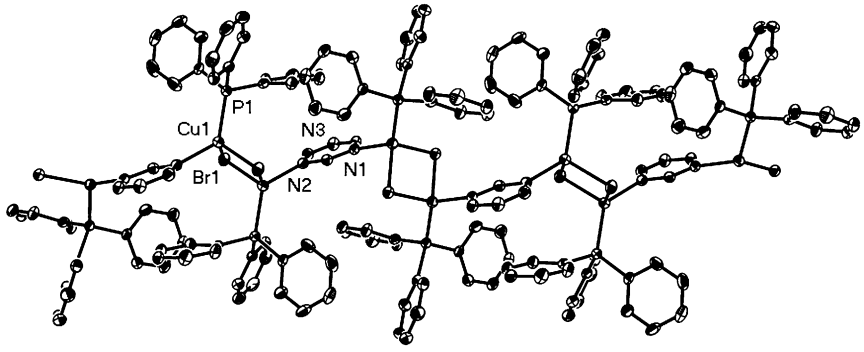

Fig. 4. Molecular structure of $[(CuBr(PPh_3))_2(Trz)]$. Thermal ellipsoids shown at 50%. Hydrogen atoms omitted for clarity.

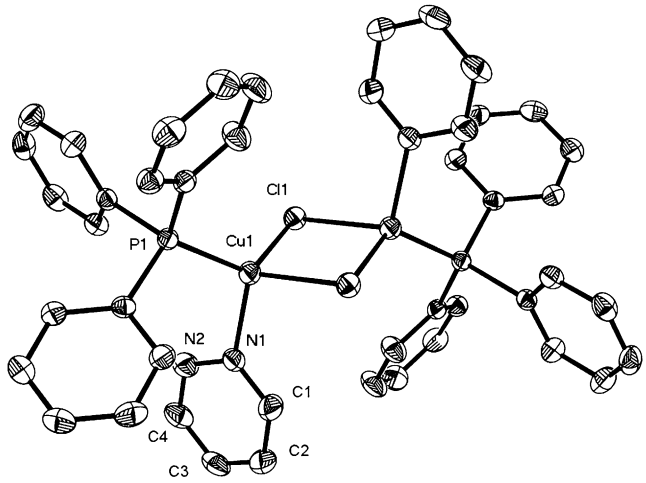

Fig. 5. Molecular structure of $[CuCl(PPh)_3(Pdz)]$. Thermal ellipsoids shown at 50%. Hydrogen atoms omitted for clarity.

Putative polymeric structures for $[(CuCl(P(OPh)_3))_3(Trz)]$

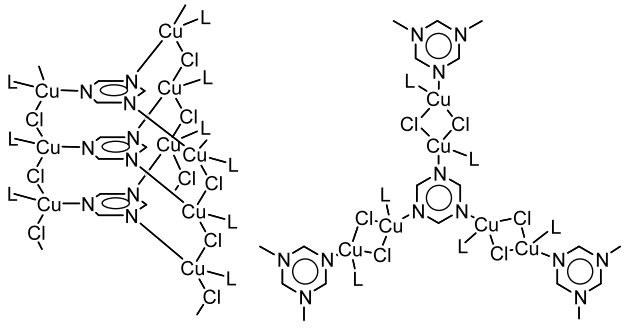

Actual hexameric structure of $[(CuCl(P(OPh)_3))_3(Trz)]$

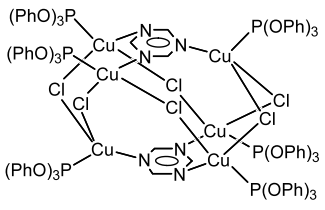

Chart 3.

hexamer structure, the Cu–N bonds form angles of 9.6°–16.9° with the triazine planes. The six copper atoms form a trigonally distorted octahedron, as do the six nitrogen and the six phosphorus atoms, respectively. The 'top' and 'bottom' Cu_3 planes are separated by only 2.654, 2.610 Å; other pairings of Cu_3 planes lie about 4.63 Å apart. A central void, roughly 7.3 Å across by 3.0 Å high, is apparent in space filling projection of the hexamer core. Presumably, a combination of the trigonal templating effect of the triazine molecules and size of the triphenyl phosphite ligands results in the formation of a compact core with peripheral phosphites.

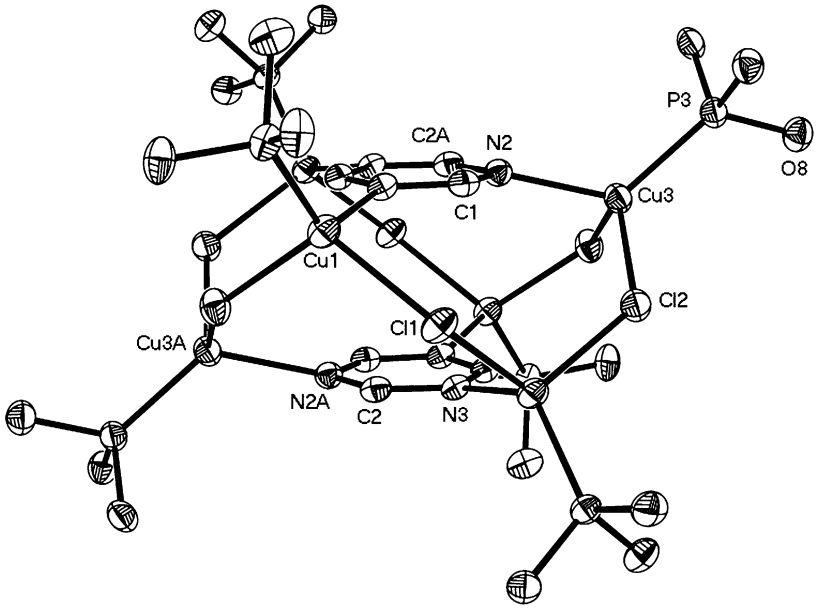

Fig. 6. Molecular structure of $[(CuCl(P(OPh)_3))_3(Trz)]$. Thermal ellipsoids shown at 50%. Phenyl rings and hydrogen atoms omitted for clarity.

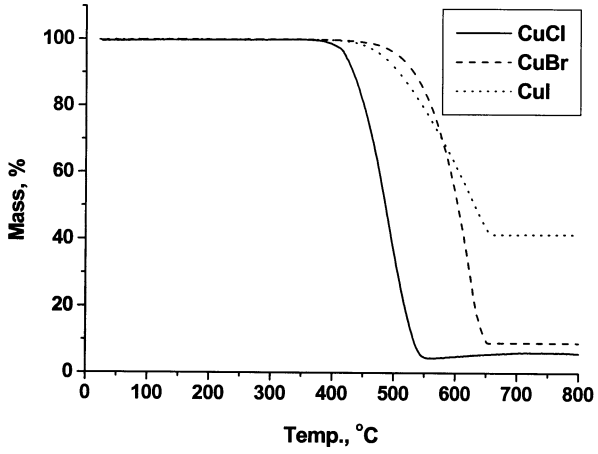

Fig. 7. Thermogravimetric mass loss profiles of CuX (X = Cl, Br, I).

Triazine templating is also evident in the channelled structure of $[(CuBr)_2(Trz)]$ [4].

3.3. Thermogravimetry

TGA (5° min^{-1}, 25–900 °C, 40 ml min^{-1} N_2) has proved to be a very effective tool for confirming the stoichiometry of CuX–B complexes, as well as aiding in the identification of metastable, more copper-rich phases [1,17,22]. For comparison purposes, the thermal behavior of the CuX salts was examined (see Fig. 7). The TGA decomposition of these materials does not produce copper metal or other identifiable material. The final mass percent (6% for CuCl, 9% for CuBr, and 42% for CuI) lies between that of CuX and Cu, suggesting a probable mixture of the two. Nevertheless, the mass loss percentage following formation of CuX remains essentially constant, regardless of the original source.

The results of TGA for complexes without L are provided in Table 5 and several representative TGA traces are shown in Figs. 8 and 9. The 1:1 complexes all showed an initial mass loss corresponding to loss of half an equivalent of B ligand. This loss occurred at modest temperatures, commencing at about 100–140 °C, and resulted in a stoichiometry ($CuXB_{1/2}$), which corresponds well to that of the 2:1 complexes, $(CuX)_2B$. In the 185–205 °C range, the 2:1 intermediates further decomposed to form CuX. Similar behavior has been observed for Pyz and Bpy complexes [1,17,22]. Although shallow plateaus suggest the possible existence of metastable intermediate phases, $[(CuX)_4(Pdz)]$ (X = Cl, Br), careful studies of Bpy complexes by Nather et al. [17] have afforded no evidence for such 4:1 species. The overall sequence for the 1:1 complexes is illustrated by reactions (2) and (3).

$$CuXB \rightarrow 1/2\ (CuX)_2B + 1/2\ B \quad (2)$$

$$(CuX)_2B \rightarrow 2CuX + B \quad (3)$$

In general, the TGA results for the 2:1 complexes of the bidentate B ligands reflected decomposition steps corresponding to the later stages of the 1:1 sequence (reaction (3)). Thus, the TGA results for $[(CuI)_2(Pdz)]$ were roughly identical to those of [CuI(Pdz)] following the initial loss of 1/2 equiv. of Pdz (Fig. 8). Also consistent with Eq. (3), most of the 2:1 complexes decomposed directly to CuX, beginning 125–220 °C. The thermal behavior of the unique complex $[(CuCl)_3(Ptz)_2]$ was complicated. However, possible intermediates $[(CuCl)_2(Ptz)]$ and $[(CuCl)_3(Ptz)]$ were suggested by the data. The 3:2 → 2:1 → 3:1 sequence is

Table 5
Thermogravimetric decomposition results for CuX–B complexes

Complex	Temperature (°C)	Product	wt.% (theory)	wt.% (actual)
$[(CuCl)_2(Pym)]$	135–210	CuCl	71	71
$[(CuBr)_2(Pym)]$	145–255	CuBr	78	78
$[(CuI)_2(Pym)]$	155–235	CuI	83	83
[CuCl(Qnz)]	135–205	$[(CuCl)_2(Qnz)]$	72	73
	205–260	CuCl	43	46
[CuBr(Qnz)]	140–195	$[(CuBr)_2(Qnz)]$	76	77
	195–270	CuBr	52	54
$[(CuI)_2(Qnz)]$	170–265	CuI	75	75
[CuCl(Pdz)]	100–185	$[(CuCl)_2(Pdz)]$	78	78
	185–230	$[(CuCl)_4(Pdz)]$?	66	69
	230–425	CuCl	55	55
[CuBr(Pdz)]	120–195	$[(CuBr)_2(Pdz)]$	82	83
	195–260	$[(CuBr)_4(Pdz)]$?	73	74
	260–470	CuBr	64	68
[CuI(Pdz)]	110–200	$[(CuI)_2(Pdz)]$	85	83
	200–250	CuI	70	71
$[(CuI)_2(Pdz)]$	170–250	CuI	83	83
$[(CuCl)_3(Ptz)_2]$	130–235	$[(CuCl)_2(Ptz)]$	88	89
	235–305	$[(CuCl)_3(Ptz)]$	77	75
[CuBr(Ptz)]	205–245	$[(CuBr)_2(Ptz)]$	76	81
	245–315	??		70
$[(CuI)_2(Ptz)]$	220–310	$[(CuI)_4(Ptz)]$?	87	86
$[(CuCl)_2(Trz)]$	110–160	$[(CuCl)_3(Trz)]$	91	90
	160–230	CuCl	71	72
$[(CuCl)_3(Trz)]$	120–175	$[(CuCl)_4(Trz)]$?	95	96
	175–250	CuCl	79	77
$[(CuBr)_3(Trz)_2]$	90–150	$[(CuBr)_2(Trz)]$	97	94
	145–175	$[(CuBr)_3(Trz)]$	92	89
	175–250	CuBr	78	77
$[(CuBr)_2(Trz)]$	105–165	$[(CuBr)_3(Trz)]$	93	93
	165–220	CuBr	78	79
$[(CuBr)_3(Trz)]$	75–150	$[(CuBr)_6(Trz)]$?	92	95
	150–235	CuBr	84	82
$[(CuI)_2(Trz)]$	125–200	CuI	82	82

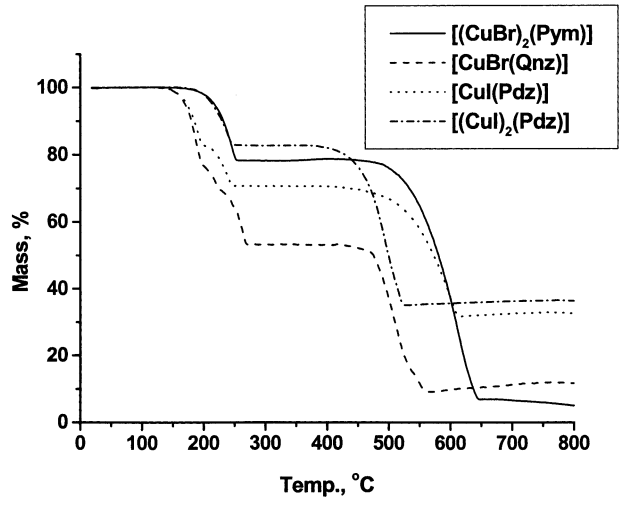

Fig. 8. Thermogravimetric mass loss profiles of selected Pym, Qnz, and Pdz complexes.

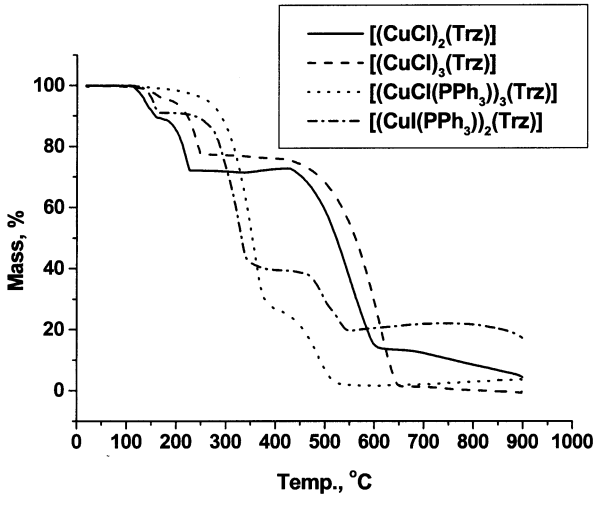

Fig. 9. Thermogravimetric mass loss profiles of selected Trz complexes.

Table 6
Thermogravimetric decomposition results for CuX–L–B complexes

Complex	Temperature (°C)	Product	wt.% (theory)	wt.% (actual)
$[(CuCl(PPh_3))_2(Pym)]$	115–175	$[(CuCl(PPh_3))_8(Pym)]$?	98	97
	245–355	CuCl	25	28
$[(CuBr(PPh_3))_2(Pym)]$	75–175	$[(CuBr(PPh_3))_4(Pym)]$?	96	95
	175–380	CuBr	32	30
$[(CuI(PPh_3))_2(Pym)]$	145–170	$[CuI(PPh_3)]$	92	92
	255–325	CuI	39	40
$[(CuCl(P(OPh)_3))_2(Pym)]$	105–210	$[CuCl(P(OPh)_3)]$	91	91
	210–350	CuCl	22	23
$[(CuBr(P(OPh)_3))_2(Pym)]$	100–190	$[CuBr(P(OPh)_3)]$	92	91
	190–280	CuBr	29	32
$[(CuCl(PPh_3))_2(Qnz)]$	120–195	$[CuCl(PPh_3)]$	85	88
	195–350	CuCl	23	24
$[(CuBr(PPh_3))_2(Qnz)]$	160–210	$[CuBr(PPh_3)]$	86	85
	210–340	CuBr	31	31
$[(CuI(PPh_3))_8(Qnz)]$	120–170	$[CuI(PPh_3)]$	96	96
	170–325	CuI	41	42
$[(CuCl(P(OPh)_3))_2(Qnz)]$	125–280	CuCl	21	24
$[(CuBr(P(OPh)_3))_2(Qnz)]$	135–285	CuBr	28	30
$[(CuCl(PPh_3))_2(Pdz)]$	115–180	$[CuCl(PPh_3)]$	90	92
	180–400	CuCl	24	25
$[CuBr(PPh_3)(Pdz)]$	65–95	$[(CuBr(PPh_3))_2(Pdz)]$	92	94
	130–200	$[CuBr(PPh_3)]$	84	79
	260–370	CuBr	30	31
$[CuI(PPh_3)(Pdz)]$	70–110	$[(CuI(PPh_3))_2(Pdz)]$	92	92
	110–160	$[CuI(PPh_3)]$	85	88
	200–380	CuI	36	35
$[CuCl(P(OPh)_3)(Pdz)]$	45–280	CuCl	20	24
$[CuBr(P(OPh)_3)(Pdz)]$	85–265	CuBr	27	32
$[(CuCl(PPh_3))_2(Ptz)]$	145–220	$[CuCl(PPh_3)]$	85	86
	220–360	CuCl	23	25
$[CuBr(PPh_3)(Ptz)]$	180–210	$[(CuBr(PPh_3))_2(Ptz)]$	88	87
	210–245	$[CuBr(PPh_3)]$	76	77
	245–340	CuBr	27	33
$[CuI(PPh_3)(Ptz)]$	165–200	$[(CuI(PPh_3))_2(Ptz)]$	89	88
	200–260	$[CuI(PPh_3)]$	78	75
	260–320	CuI	33	36
$[CuCl(P(OPh)_3)(Ptz)]$	60–90	??		94
	130–260	??		43
$[(CuBr(P(OPh)_3))_2(Ptz)]$	165–280	$[(CuBr)_2(Ptz)]$	40	43
$[(CuCl(PPh_3))_3(Trz)]$	135–390	CuCl	25	28
$[(CuBr(PPh_3))_2(Trz)]$	115–150	$[CuBr(PPh_3)]$	91	91
	240–370	CuBr	32	37
$[(CuI(PPh_3))_2(Trz)]$	120–165	$[CuI(PPh_3)]$	92	91
	165–440	CuI	39	39
$[(CuCl(P(OPh)_3))_3(Trz)]$	40–90	$[CuCl(P(OPh)_3)]$	94	94
	170–290	CuCl	23	23
$[(CuBr(P(OPh)_3))_2(Trz)]$	65–185	$[CuBr(P(OPh)_3)]$	92	91
	185–275	CuBr	29	32
$[(CuI(P(OPh)_3))_3(Trz)]$	30–150	$[CuI(P(OPh)_3)]$	95	94
	150–255	CuI	36	38

similar that of $[(CuBr)_3(Trz)_2]$, shown below in Eqs. (4) and (5).

The TGA data for the phosphorus-free complexes of the Trz (Fig. 9) proved useful in supporting elemental analysis data. A 3:2 complex, $[(CuBr)_3(Trz)_2]$, showed decomposition steps corresponding to those shown in Eqs. (4)–(6).

$$[(CuX)_3(Trz)_2] \rightarrow 3/2\ [(CuX)_2(Trz)] + 1/2\ Trz \quad (4)$$

$$[(CuX)_2(Trz)] \rightarrow 2/3\ [(CuX)_3(Trz)] + 1/3\ Trz \quad (5)$$

$$[(CuX)_3(Trz)] \rightarrow 3CuX + Trz \quad (6)$$

Similarly, the behavior of the isolated 2:1 complexes was consistent with Eqs. (5) and (6). The isolated 3:1 materials (X = Cl, Br) decomposed to form CuX (reac-

tion (6)), but also showed evidence of shallow plateaus, possibly corresponding to more copper-rich stoichiometries.

Thermogravimetry of complexes bearing $L = PPh_3$ and $P(OPh)_3$ suggested that the dimeric 1:1:1 species, [(CuXL)B] (B = Pdz, Ptz), usually underwent the sequence of reactions (7)–(9). The data are summarized in Table 6. However, when $L = P(OPh)_3$, intermediates were not usually seen.

$$(CuXL)B \rightarrow 1/2\ (CuXL)_2B + 1/2\ B \quad (7)$$

$$(CuXL)_2B \rightarrow 2CuXL + B \quad (8)$$

$$CuXL \rightarrow CuX + L \quad (9)$$

The 1:1:1 complex of CuCl–$P(OPh)_3$–Ptz yielded TGA traces that were not readily interpretible. As would be expected, the 2:2:1 complexes, $[(CuXL)_2B]$ (B = Pym, Qnz, Pdz, Ptz, Trz), typically degraded according to reactions (8) and (9). In two cases, shallow plateaus corresponded to possible metastable species $[(CuX(PPh_3))_4(Pym)]$ (X = Cl, Br) during step (8) decomposition. Support for the higher stoichiometry is provided by the isolation of $[(CuI(PPh_3))_8(Qnz)]$. The TGA trace of the latter complex showed direct decomposition to $CuI(PPh_3)$. The 3:3:1 Trz complexes bearing $P(OPh)_3$ commenced decomposition at only slightly elevated temperatures, and like the 2:2:1 species, produced CuXL.

4. Conclusions

Preparation of CuX–B complexes of Pym, Qnz, Pdz, Ptz, and Trz has revealed a rich array of stoichiometries in the polymeric products: 1:1, 3:2, 2:1, and 3:1 (Trz only). Combination of these components in the presence of PPh_3 or $P(OPh)_3$ usually produces polymeric 2:2:1 products, but can yield dimeric 1:1:1 complexes for the *ortho*-diazines Pdz and Ptz and hexameric 3:3:1 complexes for Trz.

5. Supplementary material

Crystallographic data have been deposited with the Cambridge Crystallographic Data Centre, CCDC Nos. 181168, 191279–191282 for the compounds $[(CuCl(P(OPh)_3))_3(Trz)]$, [CuBr(Qnz)], $[CuCl(PPh_3)(Pdz)]$, $[(CuBr(PPh_3))_2(Pym)]$ and $[(CuBr(PPh_3))_2(Trz)]$, respectively. Copies of these data may be obtained free of charge via http://www.ccdc.cam.ac.uk/conts/retrieving.html (or from the Director, CCDC, 12 Union Road, Cambridge, CB2 1EZ, UK (fax: +44-1223-336033; e-mail: deposit@ccdc.cam.ac.uk)).

Acknowledgements

We gratefully acknowledge support from the Henry Dreyfus Teacher-Scholar Awards Program of the Camille and Henry Dreyfus Foundation (TH-99-010), the Petroleum Research Fund of the American Chemical Society (32226-B3), and the Thomas F. and Kate Miller Jeffress Memorial Trust (J-440). We also acknowledge the following partial support: a Verizon Summer Research Fellowship (B.D.B.) and a semester research assignment from the College of William & Mary (R.D.P.). We are indebted to NSF (CHE-9808165) and Clemson University for the purchase of CCD diffractometer (W.T.P. and M.K.).

References

[1] (a) P.M. Graham, R.D. Pike, M. Sabat, R.D. Bailey, W.T. Pennington, Inorg. Chem. 39 (2000) 5121;
(b) R.D. Pike, P.M. Graham, K.A. Guy, T.J. Johnson, J.R. Cole, S.M. Stamps, L.E. Klemmer, J. Chem. Educ. 78 (2001) 1522.
[2] (a) M.J. Begley, O. Eisenstein, P. Hubberstey, S. Jackson, C.E. Russell, P.H. Walton, J. Chem. Soc., Dalton Trans. (1994) 1935;
(b) M. Munakata, T. Kuroda-Sowa, M. Maekawa, A. Honda, S. Kitagawa, J. Chem. Soc., Dalton Trans. (1994) 2771;
(c) O.M. Yaghi, G. Li, Angew. Chem., Int. Ed. Engl. 34 (1995) 207;
(d) J.M. Moreno, J. Suarez-Varela, E. Colacio, J.C. Avila-Roson, M.A. Hildago, D. Martin-Ramos, Can. J. Chem. 73 (1995) 1591;
(e) M. Munakata, L.P. Wu, T. Kuroda-Sowa, M. Maekawa, Y. Suenaga, S. Nakagawa, J. Chem. Soc., Dalton Trans. (1996) 1525;
(f) D.J.R. Brook, V. Lynch, B. Conklin, M.A. Fox, J. Am. Chem. Soc. 119 (1997) 5155;
(g) S. Kawata, S. Kitagawa, H. Kumagai, S. Iwabuchi, M. Katada, Inorg. Chim. Acta 267 (1998) 143;
(h) H.-K. Fun, S.S.S. Raj, R.-G. Xiong, J.-L. Zuo, Z. Yu, X.-L. Zhu, X.-Z. You, J. Chem. Soc., Dalton Trans. (1999) 1711.
[3] T. Kromp, W.S. Sheldrick, Z. Naturforsch., Teil B 54 (1999) 1175.
[4] (a) A.J. Blake, N.R. Brooks, N.R. Champness, L.R. Hanton, P. Hubberstey, M. Schroder, Pure Appl. Chem. 70 (1998) 2351;
(b) A.J. Blake, N.R. Brooks, N.R. Champness, P.A. Cook, A.M. Deveson, D. Fenske, P. Hubberstey, W.-S. Li, M. Schroder, J. Chem. Soc., Dalton Trans. (1999) 2103.
[5] (a) M. Henary, J.L. Wootton, S.I. Khan, J.I. Zink, Inorg. Chem. 36 (1997) 796;
(b) M. Munakata, L.P. Wu, T. Kuroda-Sowa, M. Maekawa, Y. Suenaga, S. Nakagawa, J. Chem. Soc., Dalton Trans. (1996) 1525;
(c) J. Lu, G. Crisci, T. Niu, A.J. Jacobson, Inorg. Chem. 36 (1997) 5140;
(d) P.-J. Prest, J.S. Moore, Acta Crystallogr., Sect. C 52 (1996) 2176.
[6] O. Teichert, W.S. Sheldrick, Z. Anorg. Allg. Chem. 626 (2000) 2196.
[7] D.T. Cromer, A.C. Larson, Acta Crystallogr., Sect. B 38 (1972) 1052.
[8] S.W. Keller, Angew. Chem., Int. Ed. Engl. 36 (1997) 247.
[9] M.J. Begley, P. Hubberstey, C.E. Russell, P.H. Walton, J. Chem. Soc., Dalton Trans. (1994) 2483.
[10] M. Maekawa, M. Munakata, T. Kuroda-Sowa, Y. Nozaka, J. Chem. Soc., Dalton Trans. (1994) 603.
[11] SAINT+, Bruker Analytical X-ray Systems, Madison, WI, 1997.
[12] SADABS, Bruker Analytical X-ray Systems, Madison, WI, 1997.

[13] CRYSTAL CLEAR, Rigaku Corporation, 1999.
[14] GEMINI, Bruker Analytical X-ray Systems, Madison, WI, 1997.
[15] G.M. Sheldrick, SHELXTL, Crystallographic Computing System, Version 5.1, Bruker Analytical X-ray Systems, Madison, WI, 1997.
[16] S. Kawata, S. Kitagawa, H. Kumagai, S. Iwabuchi, M. Katada, Inorg. Chim. Acta 267 (1998) 143.
[17] C. Nather, I. Jess, J. Greve, Polyhedron 20 (2001) 1017.
[18] J.Y. Lu, B.R. Cabrera, R.-J. Wang, J. Li, Inorg. Chem. 38 (1999) 4608.
[19] R.D. Pike, W.H. Starnes, Jr., G.B. Carpenter, Acta Crystallogr., Sect. C 55 (1999) 162 (and references therein).
[20] (a) J.A. Campbell, C.L. Raston, A.H. White, Aust. J. Chem. 30 (1977) 1937;
(b) M.R. Churchill, R.J. Rotella, Inorg. Chem. 18 (1979) 166;
(c) P.C. Healy, C. Pakawatchai, C.L. Raston, B.W. Skelton, A.H. White, J. Chem. Soc., Dalton Trans. (1983) 1905;
(d) P.C. Healy, C. Pakawatchai, A.H. White, J. Chem. Soc., Dalton Trans. (1983) 1917;
(e) J.C. Dyason, L.M. Engelhardt, P.C. Healy, A.H. White, Aust. J. Chem. 37 (1984) 2201;
(f) L.M. Engelhardt, R.I. Papasergio, P.C. Healy, A.H. White, Aust. J. Chem. 37 (1984) 2206;
(g) J.C. Dyason, L.M. Engelhardt, C. Pakawatchai, P.C. Healy, A.H. White, Aust. J. Chem. 38 (1985) 1247;
(h) J.C. Dyason, L.M. Engelhardt, P.C. Healy, C. Pakawatchai, A.H. White, Inorg. Chem. 24 (1985) 1950;
(i) N.P. Rath, E.M. Holt, K. Tanimura, J. Chem. Soc., Dalton Trans. (1986) 2303;
(j) P.C. Healy, J.D. Kildea, A.H. White, Aust. J. Chem. 42 (1989) 2206.
[21] R.D. Pike, B.D. Borne, J.T. Maeyer, A.L. Rheingold, Inorg. Chem. 41 (2002) 631.
[22] (a) C. Nather, I. Jess, Monat. Chem. 132 (2001) 897;
(b) C. Nather, I. Jess, H. Studzinski, Z. Naturforsch., Teil B 56 (2001) 997.